Effect of land albedo, CO2, orography, and oceanic heat transport on extreme climates

V. Romanova, G. Lohmann, K. Grosfeld

Clim. Past, 2, 31–42, 2006
www.clim-past.net/2/31/2006/

Climate of the Past

Effect of land albedo, CO_2, orography, and oceanic heat transport on extreme climates

V. Romanova[1], **G. Lohmann**[2,3], **and K. Grosfeld**[2,3]

[1]Institute of Oceanography, University of Hamburg, 20146 Hamburg, Germany
[2]Alfred Wegener Institute for Polar and Marine Research, 27515 Bremerhaven, Germany
[3]Department of Physics, University of Bremen, Otto-Hahn-Allee, 330440 Bremen, Germany

Received: 11 October 2005 – Published in Clim. Past Discuss.: 7 December 2005
Revised: 2 June 2006 – Accepted: 2 June 2006 – Published: 30 June 2006

Abstract. Using an atmospheric general circulation model of intermediate complexity coupled to a sea ice – slab ocean model, we perform a number of sensitivity experiments under present-day orbital conditions and geographical distribution to assess the possibility that land albedo, atmospheric CO_2, orography and oceanic heat transport may cause an ice-covered Earth. Changing only one boundary or initial condition, the model produces solutions with at least some ice-free oceans in the low latitudes. Using some combination of these forcing parameters, a full Earth's glaciation is obtained. We find that the most significant factor leading to an ice-covered Earth is the high land albedo in combination with initial temperatures set equal to the freezing point. Oceanic heat transport and orography play only a minor role for the climate state. Extremely low concentrations of CO_2 also appear to be insufficient to provoke a runaway ice-albedo feedback, but the strong deviations in surface air temperatures in the Northern Hemisphere point to the existence of a strong nonlinearity in the system. Finally, we argue that the initial condition determines whether the system can go into a completely ice covered state, indicating multiple equilibria, a feature known from simple energy balance models.

1 Introduction

Investigations of glacial carbonate deposits suggest a sequence of extreme Neoproterozoic climate events (600–800 million years ago). Paleolatitude indicators and paleomagnetic data (Hoffman, et al., 1998; Schmidt and Williams, 1995; Sohl et al., 1999; Evans et al., 2000) imply widespread equatorial glaciation at sea level. It was hypothesised that the Earth was completely ice covered (Kirschvink, 1992; Hoffman et al., 1998; Kirschvink et al., 2000; Hoffman and Schrag, 2002). Still, the question remains, whether the Earth was completely ice covered ("hard snowball" Earth) or some tropical ocean areas remained ice free ("slushball" Earth), and which mechanism drove the climate system into the glaciated state and which allowed the escape from it (Caldeira and Kasting, 1992). Such extreme climates in the Earth's history provide the motivation to investigate under what conditions the climate system is susceptible to extreme changes.

Fraedrich et al. (1999) and Kleidon et al. (2000) used a general circulation model to investigate the land albedo effect of homogeneous vegetation extremes – global desert and global forest. It was found that the dominant signal is related to changes in the hydrological cycle and that the altered water and heat balance at the surface has a potential impact on regional climate. Kubatzki and Claussen (1998) and Wyputta and McAvaney (2001) showed that during the Last Glacial Maximum (LGM) the land albedo increased by 4% due to vegetation changes. In addition to this, the influence of the mountain chains and highly elevated glaciers with strong ice albedo feedback leads to large climate anomalies and an alteration of the atmospheric circulation and precipitation patterns (Lorenz et al., 1996; Lohmann and Lorenz, 2000; Romanova et al., 2005). The increase of the oceanic heat transport is also considered to be a crucial factor to prevent Earth's glaciation. For example, Poulsen et al. (2001) investigated the role of the oceanic heat transport in 'snowball' Earth simulations and concluded that it could stop the southward advance of glaciers, such that a global glaciation on the Earth could not occur. Multiple stable equilibria are found in an aqua-planet simulation performed with a coupled atmospheric general circulation model with respect to change of the oceanic heat transport and initial conditions (Langen and Alexeev, 2004): one warm and ice free planet and one cold and icy climatic state. Furthermore, the atmospheric CO_2 level could also lead to a climate instability and a runaway sea-ice albedo mechanism (Poulsen, 2003). The magnitude

Correspondence to: V. Romanova
(romanova@ifm.uni-hamburg.de)

Published by Copernicus GmbH on behalf of the European Geosciences Union.

of the atmospheric greenhouse gas concentrations, causing glaciation, is still under intense debate (e.g. Chandler and Sohl, 2000; Donnadieu et al., 2004).

In this study, we are interested in the sensitivity of the climate to changes of the land albedo, orography, oceanic heat transport and CO_2 concentration. Using an AGCM of intermediate complexity we investigate the climate response to some extreme configurations of the boundary conditions. Therefore, we perform numerical experiments with different land albedo values and analyse scenarios, in which the land is completely covered with oak forests or glaciers. We have chosen sensitivity experiments with extreme orographical and oceanic heat transport forcings, and with respect to the snowball Earth hypothesis, we vary the CO_2 concentrations to some extreme values. We left the land-sea geometry to present or to Last Glacial Maximum distributions. Most of the external parameters which are different of extreme climate states in the earth history (snowball Earth) are held fixed in order to isolate the effect of land albedo, CO_2, and oceanic heat transport with fixed parameters. Our approach is therefore intended as a sensitivity study.

The paper is organized as follows: in Sect. 2 the model is briefly described and in the Sect. 3 the results are given. In Sect. 4 the results are discussed and final conclusions are given in Sect. 5.

2 Methodology

2.1 Model design

The atmospheric general circulation model (AGCM) used in our study is PUMA (Portable University Model of the Atmosphere) developed in Hamburg (Fraedrich, 1998; Lunkeit et al., 1998). It is based on the primitive equations transformed into dimensionless equations of the vertical component of absolute vorticity, the horizontal divergence, the temperature, the logarithm of the surface pressure and the specific humidity. The equations are solved using the spectral transform method (Orszag, 1970; Eliasen et al., 1970), in which the variables are represented by truncated series of spherical harmonics with wave number 21. The calculations are evaluated on a longitude/latitude grid of 64 by 32 points, which corresponds approximately to a 5.6° resolution in Gaussian grid. In the vertical direction five equally spaced, terrain-following sigma levels are used. The land and soil temperatures, soil hydrology and river runoff are parameterized in the model.

PUMA is classified as a model of intermediate complexity (Claussen et al., 2002) and it is designed to be comparable with comprehensive AGCMs like ECHAM (Roeckner et al., 1992). Previously, it was used to study stormtracks and baroclinic life cycles (e.g. Frisius et al., 1998; Franzke et al., 2000) and to investigate multidecadal atmospheric response to the North Atlantic sea surface temperatures (SST) forcing (Grosfeld et al., 2006[1]) as well as to simulate glacial climates (Romanova et al., 2005).

PUMA is coupled to a mixed layer ocean model, which allows the prognosis of the sea surface temperatures (SST). The mixed layer ocean is forced with the oceanic heat transport and its depth is fixed at 50 m. A simple zero layer thermodynamic sea ice model is also included. The temperature gradient in the sea ice is linear and eliminates the capacity of the ice to store heat. Sea ice is formed if the ocean temperature drops below the freezing point (–1.9°C), and melts whenever the ocean temperature increases above this point. The albedo for sea ice R^{ice}, glaciers R^{gl} and snow-covered areas R^{sn} is a linear function of the surface temperature,

$$R^{sn,gl} = R^{sn,gl}_{\max} + (R^{sn,gl}_{\min} - R^{sn,gl}_{\max})\frac{T_s - 263.16}{10} \quad (1)$$

$$R^{\mathrm{ice}} = \min(R^{\mathrm{ice}}_{\max}, 0.5 + 0.025(273.0 - T_i)) \quad (2)$$

where, T_s and T_i are the surface temperature over land and sea ice, respectively. The maximum albedo for sea ice is $R^{\mathrm{ice}}_{\max}$=0.7, the minimum and maximum albedo for glaciers are $R^{gl}_{\min}$=0.6 and $R^{gl}_{\max}$=0.8, and that for snow varies from $R^{sn}_{\min}$ = 0.4 to $R^{sn}_{\max}$ = 0.8. The albedo of water is set to 0.069.

2.2 Model set-up

To initialise the control run, a spin-up run (Exp_prescr, Table 1) is performed with prescribed SSTs and sea ice margins. The values of the global SST are taken to be equal to the climatological mean for the time period between 1979 and 1994 from the Atmospheric Model Intercomparison Project (AMIP) (Phillips et al., 1995). The CO_2 concentration is fixed at 360 ppm. The orography and land-sea masks are set to present-day conditions. An equilibrium state of the spin-up run is obtained after 50 model years. The calculated 10 years monthly averaged total surface heat fluxes from Exp_prescr are taken to be equal to the oceanic heat fluxes, which serve as a forcing for the mixed layer ocean model. Thus, the oceanic heat transport is prescribed for the coupled simulations and is taken to be the same for all sensitivity studies described below, except for those which investigate the impact of zero oceanic heat transport. The maximum value of the oceanic heat transport is 1.0 PW at 30° N (Butzin et al., 2003; Romanova et al., 2005; Butzin et al., 2005) and represents a realistic value for present-day conditions (Macdonald and Wunsch, 1996). The simulation, forced with the present-day heat transport and in which the albedo is simulated by the model, is called the "control run" (Exp_slab, Table 1). For all experiments, the Earth's orbital

[1]Grosfeld, K., Lohmann, G., Rimbu, N., Lunkeit, F., and Fraedrich, K.: Atmospheric multidecadal variations in the North Atlantic realm derived from proxy data, observations, and model studies, J. Geophys. Res., submitted, 2006.

Sensitivity experiments		CO2	Orography	Abbreviation
AMIP (prescribed at the surface)		360	Present-day	***Exp_prescr***
10 years averaged surface heat fluxes from exp. ***Exp_prescr***		360	Present-day	***Exp_slab (control run)***
Albedo	albedo land - 0.2 albedo ocean - 0.069	360	Present-day	***Exp_alb02***
	albedo land - 0.8 albedo ocean - 0.069			***Exp_alb08***
	albedo land: 0.8 initial temp: - 1.9° C heat transport: zero			***Exp_IP*** (ice-planet)
Sensitivity toward initial and boundary conditions	albedo land: 0.8 initial temp: - 1.9° C **heat transport: PD**	360	Present-day	***ExpIP_HfPD***
	albedo land: 0.8 **initial temp: PD** heat transport: zero			***ExpIP_iniTempPD***
	albedo land: free initial temp: - 1.9° C heat transport: zero			***ExpIP_albfree***
	Initial state ***Exp_IP*** Albedo land: free Heat transport: zero			***ExpIP_iniIP***
CO_2 – 1 ppm		1	Present-day	***Exp_1***
CO_2 - 10 ppm		10	Present-day	***Exp_10***
CO_2 - 25 ppm		25	Present-day	***Exp_25***
CO_2 - 200 ppm		200	Present-day	***Exp_200***
CO_2 - 720 ppm		720	Present-day	***Exp_720***
CO_2 - 1440 ppm		1440	Present-day	***Exp_1440***
Zero orography		360	Zero	***Exp_flat***
Glacial orography		360	(Peltier 1994)	***Exp_glac***
Zero heat transport		360	Present-day	***Exp_zero***

Table 1. Overview of numerical experiments and their set-up.

parameters are taken for the year 2000 A.D., and are calculated according to Berger (1978).

There are four groups of sensitivity experiments (Table 1):

– The first group of experiments includes sensitivity studies related to variations of the surface albedo. In Exp_alb02 the land albedo is fixed to 0.2, corresponding to a warmer than present-day Earth, in which all the continents are being forested. In Exp_alb08, the land albedo is set to 0.8, corresponding to all continents being completely covered by glaciers. One experiment is performed to simulate Earth's complete glaciation. In this experiment, called "Ice Planet" simulation (abbr. Exp_IP), the land albedo is fixed to 0.8, the oceanic heat transport is set to zero and the initial SST field is uniformly set to –1.9°C, the freezing temperature of seawater.

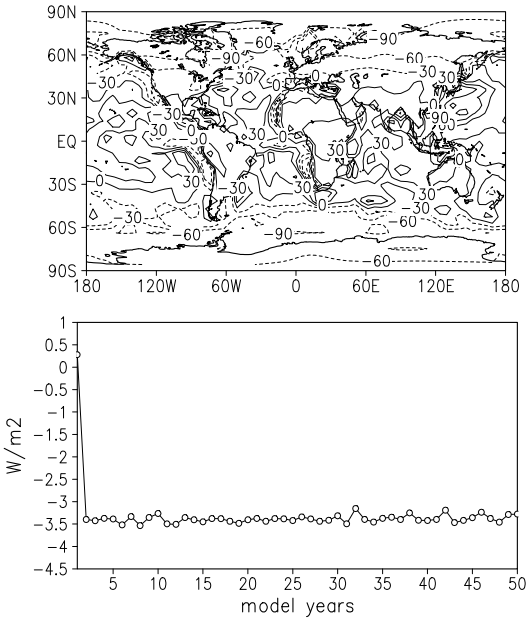

Fig. 1. The radiation balance for the control run **(a)** lon/lat plot averaged over the last 25 years of integration [W/m^2], **(b)** averaged globally versus model years.

– The second group of experiments investigates the influence of different initial and boundary conditions in the "Ice Planet" simulation. Only one initial or boundary condition is changed in each experiment. In ExpIP_HfPD the oceanic heat transport is set to that of present-day (same as control run). In experiment ExpIP_iniTempPD the initial surface temperature field is set to that from AMIP data; and in ExpIP_albfree the albedo is simulated by the model. An additional experiment ExpIP_iniIP is performed, starting from a planet covered with snow (with intermediate snow albedo of 0.6), zero heat transport and an initial temperature equal to the freezing point. This experiment is run for 6 months and then the surface albedo is allowed to be simulated by the model.

– The third group of experiments is performed to investigate the sensitivity of the climate system to carbon dioxide concentration. The experiments are run under present day boundary conditions with different atmospheric CO_2 values. The highest concentration is taken to be 4 times the present-day value of 360 ppm and the lowest is 1 ppm, corresponding to a "clear" atmosphere. In between these values, simulations are carried out with CO_2 concentrations of 10, 25, 200 and 720 ppm (abbreviated Exp_1440, Exp_720, . . ., Exp_1; Table 1).

– The fourth group of experiments investigates the sensitivity of the system related to orography and oceanic heat transport. In experiment Exp_flat, the orography

Exp. name	Global Temperature (°C) ANM	DJF	JJA	Planetary Albedo (in fraction)	Surface Albedo (in fraction)
control	17.00	15.84	18.36	0.31	0.17
Exp_alb02	18.33	17.21	19.65	0.31	0.12
Exp_alb08	-0.36	-1.26	1.10	0.41	0.39
Exp_IP	-50.58	-49.20	-52.11	0.69	0.73
ExpIP_HfPD	-50.84	-49.61	-52.23	0.69	0.73
ExpIP_iniTempPD	-1.02	-2.76	1.21	0.42	0.38
ExpIP_albfree	16.14	14.66	17.15	0.32	0.18
ExpIP_iniIP	2.94	1.23	5.17	0.39	0.33
Exp_1	-6.75	-6.73	-6.76	0.40	0.39
Exp_10	0.15	-0.50	1.35	0.37	0.33
Exp_25	7.61	6.84	8.97	0.33	0.26
Exp_200	14.25	13.03	15.85	0.32	0.20
Exp_720	19.35	18.20	20.76	0.32	0.15
Exp_1440	21.64	20.54	22.99	0.32	0.13
Exp_glac	13.96	12.54	15.80	0.33	0.23
Exp_flat	18.23	17.02	19.70	0.31	0.16
Exp_zero	16.19	14.75	17.96	0.32	0.17

Table 2. Annual mean, DJF and JJA surface air temperatures (SAT) and globally averaged surface and planetary albedo.

is taken to be zero and in the experiment Exp_glac the orography and the glacial mask are the glacial ones as given by Peltier (1994) for the LGM. In the experiment Exp_zero, oceanic heat transport of zero W/m^2 is applied to the mixed layer model (Table 1).

The experiments are integrated over 50 years, when they reach the equilibrium state. Figure 1 shows the balance between the surface heat flux and the heat flux at the top of the atmosphere for the control run (the deviation from the zero balance are due to water phase transitions and model errors, which are not included in the balance). No trend is found after the first year of the calculation, showing that the initial conditions are very close to the state of the model equilibrium. Longer integrations, up to 25 years (Fig. 4) are necessary for the experiments driven with extreme initial and forcing conditions. All results shown represent annual means averaged over the last 25 years of integration.

3 Results and analyses

3.1.1 Sensitivity related to changes of the land albedo

The annual mean spatial pattern of the surface air temperatures (SAT) for the control run, for the experiments with prescribed surface albedo of 0.2 and 0.8, and for the ice-planet simulation are shown in Fig. 2. The grey shading indicates the sea-ice coverage. A slight decrease of the land albedo to 0.2 (Exp_alb02, Fig. 2b) compared to the present day simulation (control run, Fig. 2a) leads to a global warming of around 1°C (Table 2) and a retreat of the sea-ice margin. Especially in high latitudes, the SAT increases and the sea ice retreats along the Antarctic coast. Contrary, a drastic increase of the albedo over the land to 0.8 (Fig. 2c), results in a decrease of the global annual mean SAT by about 18°C (Table 2) and the temperature at the equator of the Atlantic Ocean is less than 15°C (Fig. 2c). Sea-ice is formed closer to the equator as its margin reaches 40° N and 50° S. The experiment Exp_IP shows a full Earth glaciation. The global mean temperature falls to approximately –50°C, and over Antarctica –80°C are reached (Fig. 2d).

The calculated globally averaged surface albedo and the planetary albedo (Table 2) show that the planetary albedo is larger by 82% and 158% than the surface albedo in the control run and Exp_alb02, due to the high rates of evaporation and cloud formation. In experiment Exp_alb08 it is only 5%. In contrast to this, the surface albedo in the ice planet simulation (Exp_IP) is larger (approximately 6%) than the planetary albedo.

3.1.2 Sensitivity of the Ice Planet simulations

To isolate the effect and to determine the importance of each boundary and initial conditions, sensitivity experiments of the Ice Planet simulation are performed, holding only one of the boundary conditions the same as in the case of the control run. Changing the heat transport to present-day values, the model simulation does not generate any considerable change in the SAT pattern (Fig. 3a). The temperatures increase by only 0.26°C, but the earth remains ice covered in the equilibrium state, which is reached about 5 years later than in the Exp_IP (Fig. 4). If the initial temperature is set to present day (AMIP) values, the planet does not end in a full glaciation, although strong sea-ice formation in the Northern Hemisphere occurs and the global temperature is almost 20°C lower compared to the control run (Table 2 and Fig. 4). Leaving the land albedo free to develop in ExpIP_albfree, the global temperature increases to about 16°C (Fig. 3c) and the spatial temperature pattern tends to resemble the control run. An increase of the temperature (of about 10°C) also occurs in the experiment ExpIP_iniIP, in which the land albedo was released free to develop after 6 months of the Ice Planet integration (Fig. 3d, Fig. 4). The relation between the surface and planetary albedo in the last two sensitivity experiments is similar to the present-day conditions (the planetary albedo is larger than the surface albedo), characterised by an evaporation regime and cloud formation (Table 2).

The decrease of temperature in the first two sensitivity experiments shows that the oceanic heat transport and the initial temperature are not sufficient to prevent the global cooling. The global glaciation occurs independently of the oceanic heat transport. In contrast to this, the increased land albedo provokes the planet's warming and appears to be the most important factor for the change of the climate system.

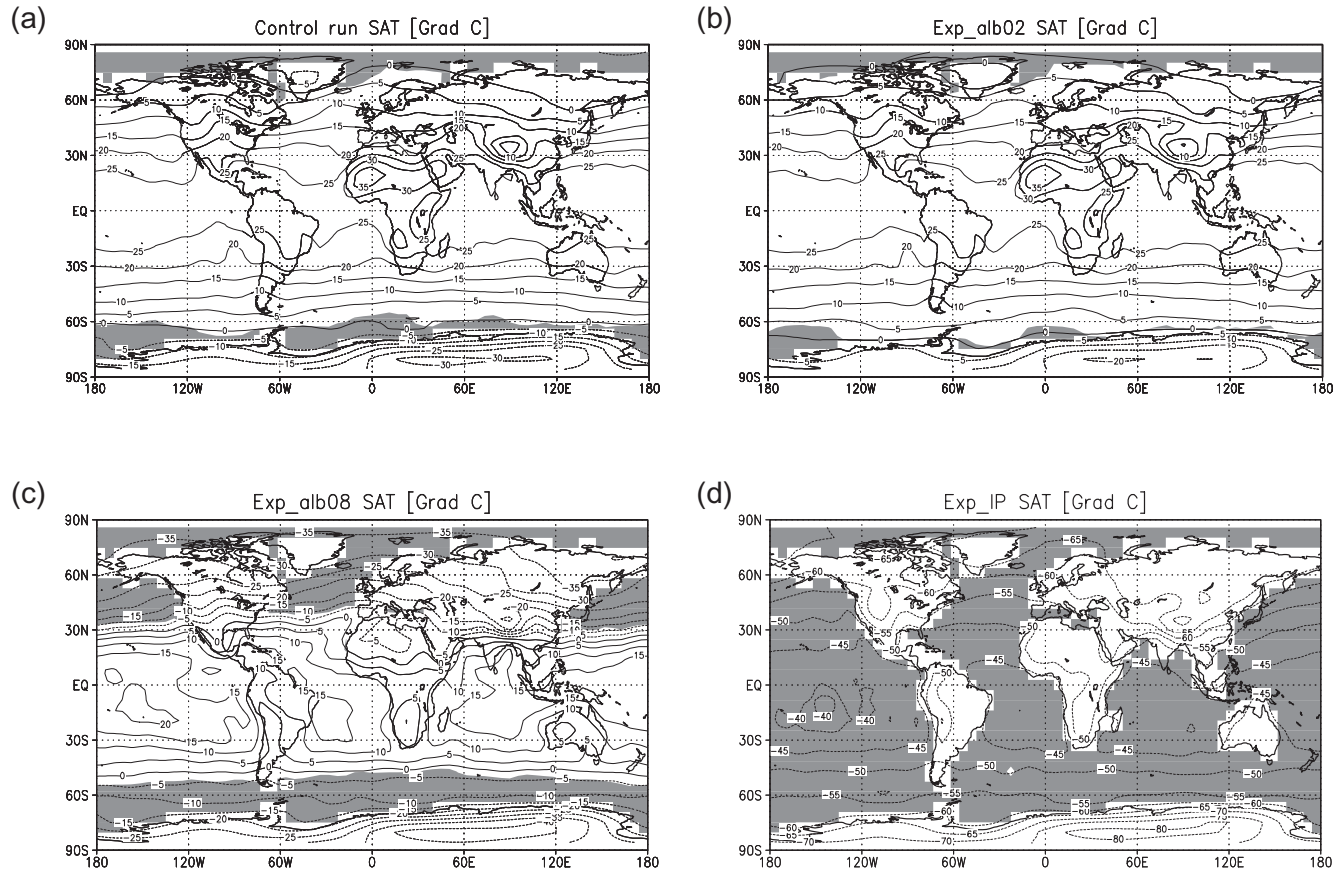

Fig. 2. Spatial pattern of the annual mean surface air temperatures averaged over a period of 25 years of integration for experiments **(a)** control run; **(b)** Exp_alb02; **(c)** Exp_alb08; and **(d)** Exp_IP (land alb. set to 0.8; initial temp. set to –1.9°C; the oceanic heat transport is zero). The grey shading indicates the annual mean sea-ice cover.

3.1.3 Sensitivity of the climate system to CO_2 concentration

A fourfold increase of CO_2 concentration relative to present-day values, results in a more than 4°C increase of the global temperature, and a two fold increase of the CO_2 concentration provokes a 2°C global warming (Table 2). Reduction of CO_2 to 1 ppm results in a global cooling of 25°C compared to the control run, yielding an annual mean SAT of –7°C in EXP_1. In Fig. 5 the SAT and the sea-ice margin evolution for experiments with CO_2 concentration of 200, 25, 10 and 1 ppm are shown. Reduction of CO_2 cools the planet, sea-ice is formed closer to the equator, and the positive ice-albedo feedback is initiated. Nevertheless, the reduction of CO_2 under present-day geography and orbital conditions is not sufficient to cause a full glaciation of the planet. The dependence of the annual mean surface temperature on the log (CO_2) shows a good linear approximation (Fig. 6) consistent to, e.g., Budyko (1982), Manabe and Bryan (1985), and Oglesby and Saltzman (1990), and is valid not only for the CO_2 values near the present day concentration but also for the extreme concentrations as 1 ppm and 1440 ppm.

3.2 Orography and oceanic heat transport

In Fig. 7 the spatial SAT pattern of the experiments investigating the role of orography and ocean heat transport are shown. Applying zero orography (EXP_flat), the simulation shows global warming of 1°C (Table 2). Over land, the impact is more obvious, as the temperature anomaly can reach up to 8°C in the Himalaya Massive and around 22°C in the Antarctic (Fig. 7a). Warming also occurs over the Pacific and almost over the entire Atlantic. Still, cooling is noted in some areas of the North Atlantic and the whole Southern ocean (up to –2°C).

The experiment forced with glacial orography (Peltier, 1994) and present-day heat transport generates cooling (globally about 3°C, Fig. 7b). Strong North American, North Atlantic, and Eurasian cooling of –16°C to –20°C is due to the highly elevated Laurentide Ice Sheet, influencing generally the atmospheric circulation pattern (Romanova et al., 2005). Along with a global cooling, an equatorial Pacific warming is found, a feature similar to that in the CLIMAP (1981) reconstruction of the Last Glacial Maximum.

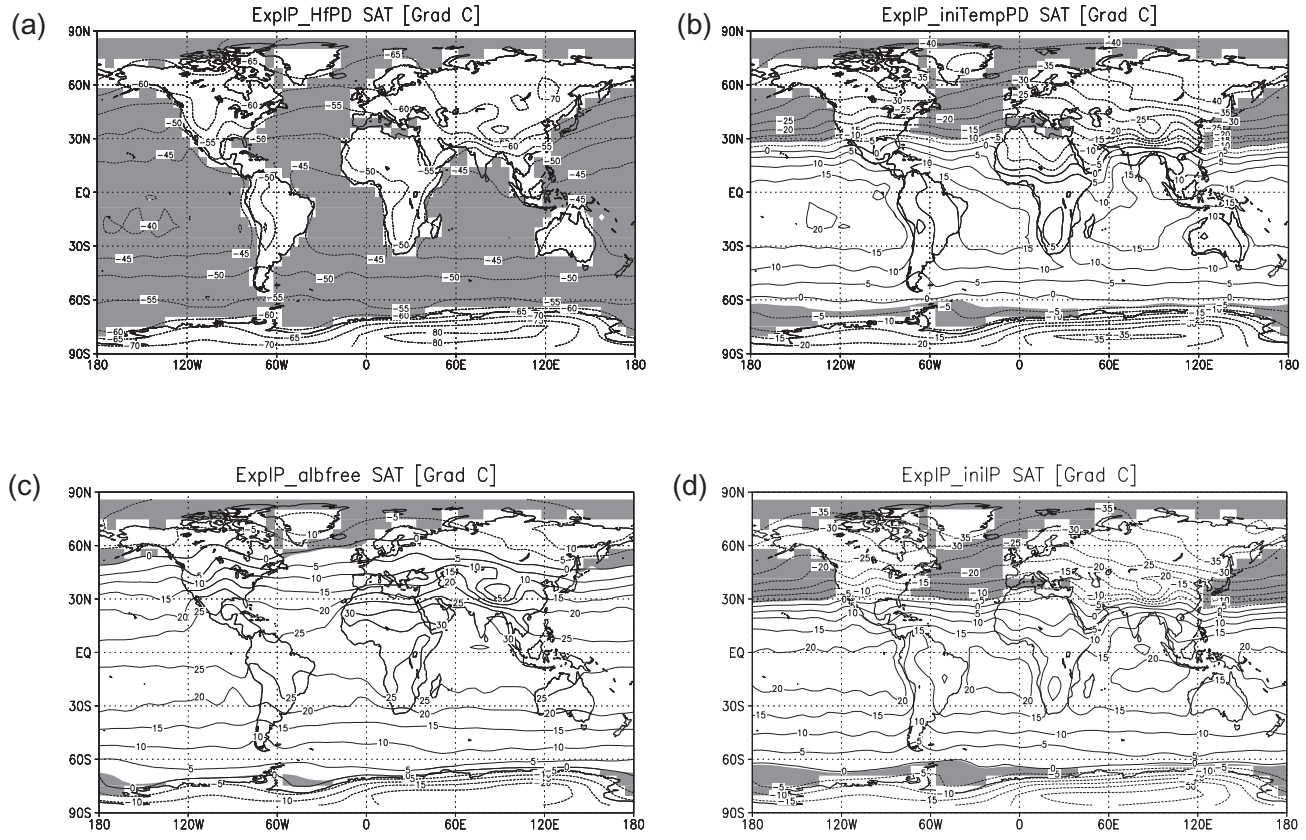

Fig. 3. As in Fig. 2, but for experiments **(a)** ExpIP_HfPD (PD heat transport); **(b)** ExpIP_iniTempPD (Pd initial temperature); **(c)** ExpIP_albfree (land alb. simulated by the model); and **(d)** ExpIP_iniIP (land alb. –0.6; zero heat transp.; initial temp. –1.9°C; after six months the albedo is released to develop) .

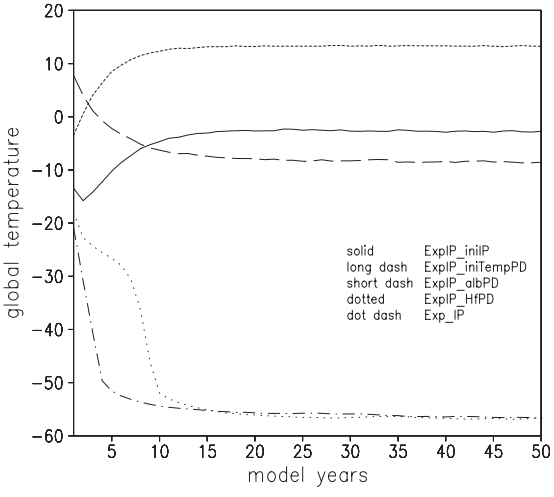

Fig. 4. Time series of global average surface temperature for ExpIP_HfPD, ExpIP_iniTempPD, ExpIP_albfree, ExpIP_iniIP and Exp_IP.

To investigating the role of the oceanic heat transport separately, we carried out an experiment, in which all boundary conditions are set equal to those in the control run and only the ocean heat transport was reduced to zero. This experiment EXP_zero shows warming in the Southern Hemisphere (SH) and cooling in the Northern Hemisphere (NH). This see-saw effect is due to a changed ocean heat redistribution. When the meridional oceanic heat transport is prohibited, the SH warms up and the heat exchange between the hemispheres is sharply reduced. A surplus of heat is found in the SH and a lack of it in the NH.

Furthermore, the sensitivity of the model to different heat transports related to different states of the glacial ocean is investigated in Romanova et al. (2006). These states are associated with CLIMAP and GLAMAP 2000 SST reconstructions (CLIMAP, 1981; Pflaumann et al., 2003). The reduction of the heat transport at 30° N is between 30% and 50% less than those in the present-day simulation (control run). The related drop in the global surface temperature is 3.5°C and 1.4°C , respectively (Fig. 3 in Romanova et al., 2006).

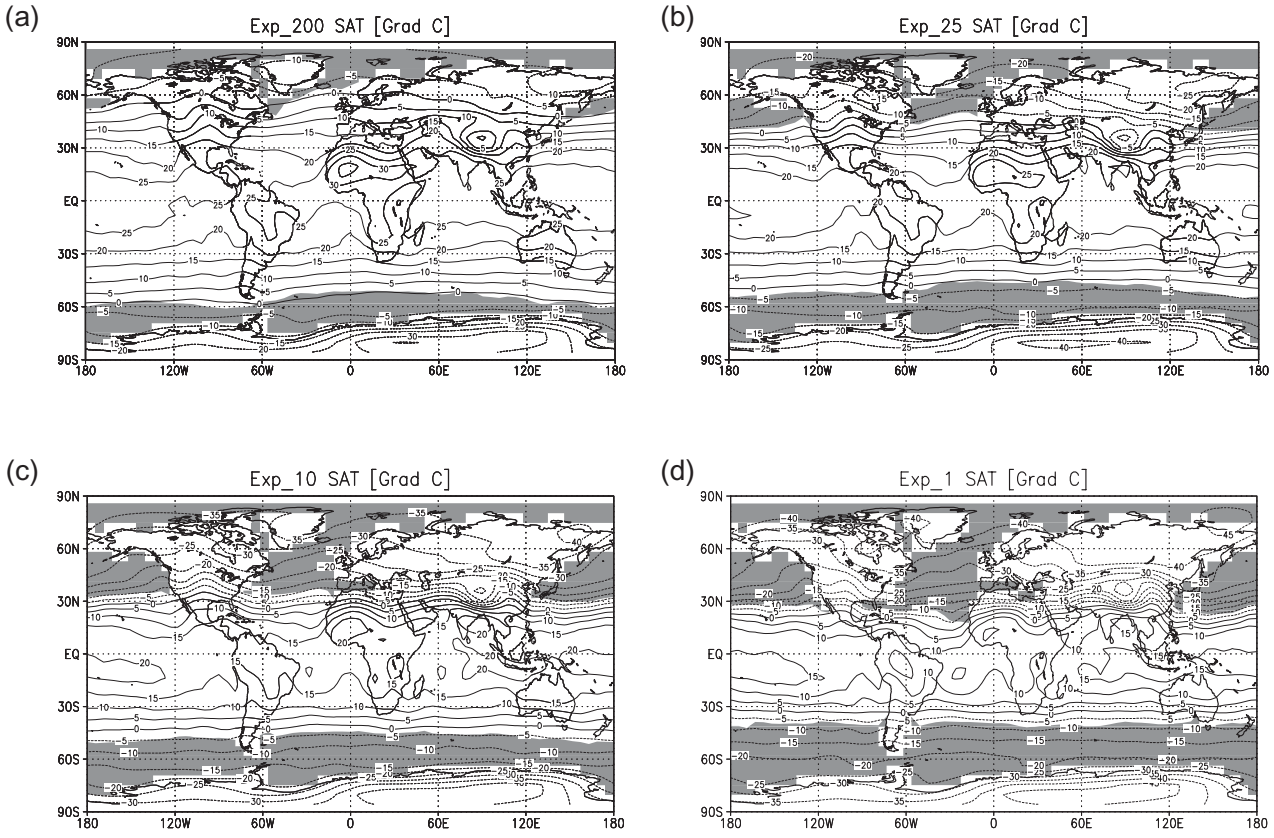

Fig. 5. As in Fig. 2, but for experiments **(a)** Exp_200; **(b)** Exp_25; **(c)** Exp_10; and **(d)** Exp_1. The numbers denote the CO_2 concentration.

3.3 Zonal mean SAT anomalies

An overview of the zonally averaged temperature anomalies relative to the control run is shown for all experiments in Fig. 8. The first panel represent the temperature anomalies for EXP_glac, EXP_flat and EXP_zero. Strong midlatitude and polar region cooling in the NH and SH, due to the extended glacial ice sheets, is found in EXP_glac. The seesaw effect between the NH and SH characterises the results of EXP_zero and an overall warming except in the Southern Ocean is found in EXP_flat. On the second panel (Fig. 8b) the SAT anomalies for the experiments with changed albedo are displayed. EXP_alb02 shows a small increase of the temperature (around 1°C) relative to the present-day simulation, except for the Antarctic, where the sharp change of surface reflectivity from glaciers (0.8) to forest (0.2) yields a warming of nearly 10°C; EXP_alb08 exhibits strong, zonal cooling up to –30°C in mid and high northern latitudes, indicating the opposite effect than in EXP_alb02 for the Antarctic; and in EXP_IP the temperature anomaly can reach –70°C in the equatorial and tropical latitudes. The third panel visualizes the temperature reduction in the NH due to the reduction of CO_2 and the consequential positive ice-albedo feedback. The extreme experiment EXP_1 exhibits very strong anomalies, up to –40°C SAT in the subtropics in the NH.

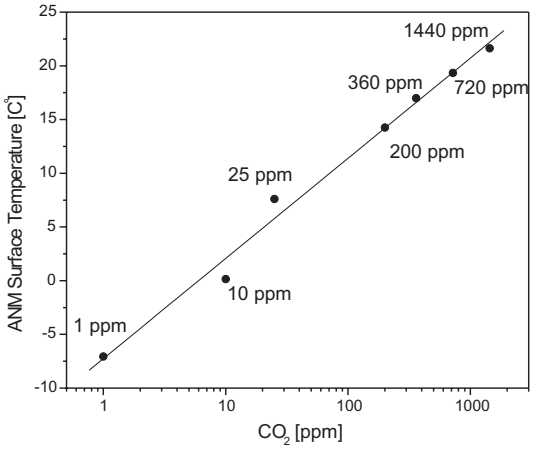

Fig. 6. Log plot of the carbon dioxide concentration versus ANM surface temperature for exp. Exp_1, Exp_10, Exp_25, Exp_200, Exp_360, Exp_720 and Exp_1440. The line shows the linear fit.

3.4 Zonal mean precipitation

To assess the Hadley circulation and the Intertropical Convergence Zone (ITCZ) for different sensitivity experiments the averaged zonal mean precipitation is calculated. The zonal

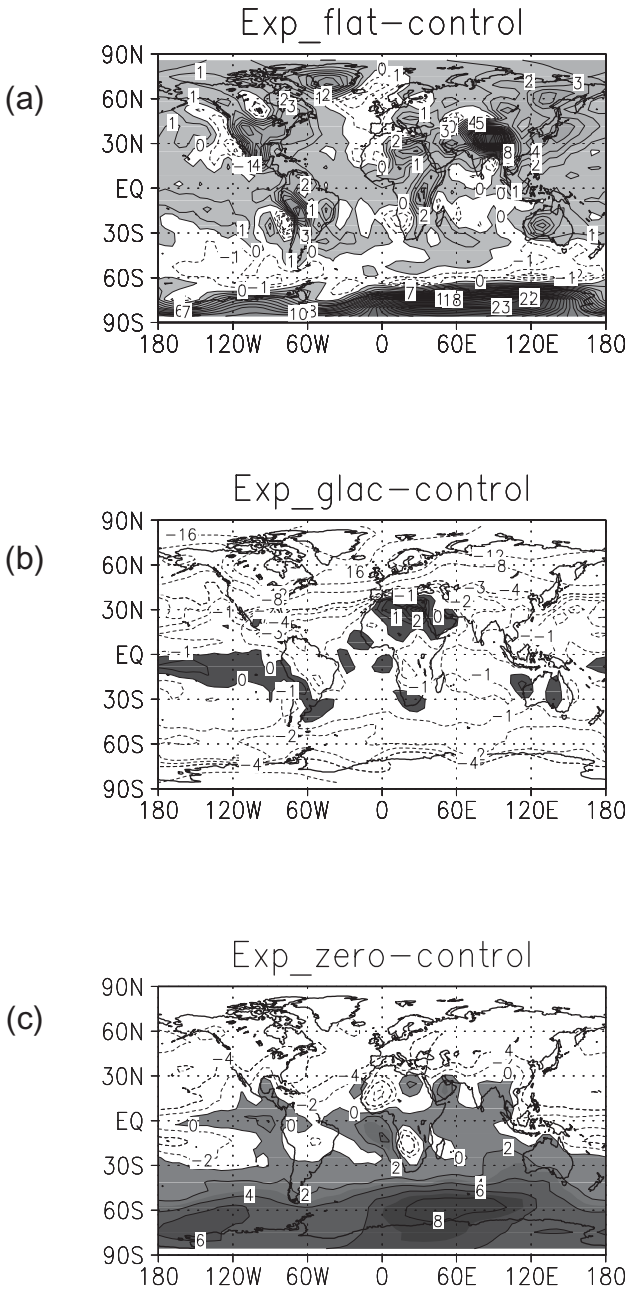

Fig. 7. Annual mean surface air temperatures anomalies: **(a)** Exp_flat-control run (zero orography); **(b)** Exp_glac-control run (LGM orography given by Peltier, 1981); and **(c)** Exp_zero-control run (zero heat transport). The grey shading indicates the positive anomalies.

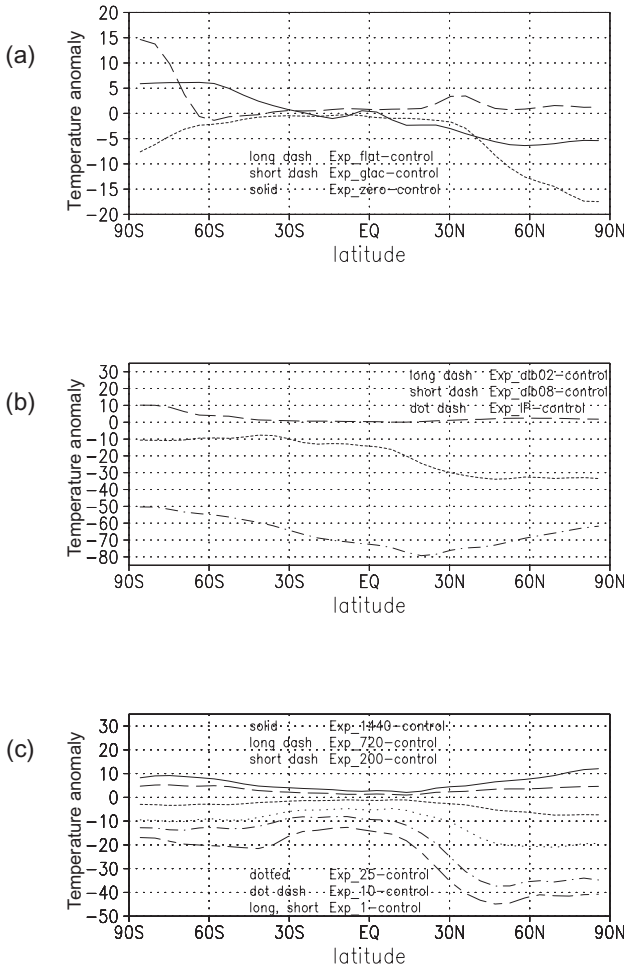

Fig. 8. Zonal mean of the global surface temperature anomalies relative to the control run: **(a)** effect of orography and oceanic heat transport; **(b)** changed land albedo and Ice Planet simulation; and **(c)** different CO_2 concentrations in the atmosphere.

mean boreal winter and summer values for the sensitivity experiments are shown in Fig. 9. The maximum precipitation in boreal winter for the present-day simulation is situated in the SH, while in the boreal summer it is located in the NH.

The experiments investigating the effect of the orography (Fig. 9a, b) EXP_flat and EXP_glac show seasonal deviations from the present-day values. In EXP_flat the maximum precipitation during boreal winter is reduced, while in EXP_glac it is enhanced. The opposite tendency is found in boreal summer, EXP_flat shows an increase in precipitation and experiment EXP_glac produces a decrease. The land elevation in the NH results in pronounced seasonality in the equatorial region. As the orography is higher, the ITCZ is strengthened in boreal winter and is suppressed in boreal summer. The absence of heat transport in EXP_zero increases the maximum precipitation in both seasons, compared to the control run.

The precipitation in the land albedo experiment EXP_alb02 is similar to the present-day's one, except in the region of Antarctica, where the drastic change of the albedo produces a peak in precipitation in winter (Fig. 9cd). In EXP_alb08 the precipitation maximum is strongly shifted to the SH (around 15° S) and located in the belt of all-years SAT maximum. The magnitude is 20% less than the present-day value. A decrease in precipitation

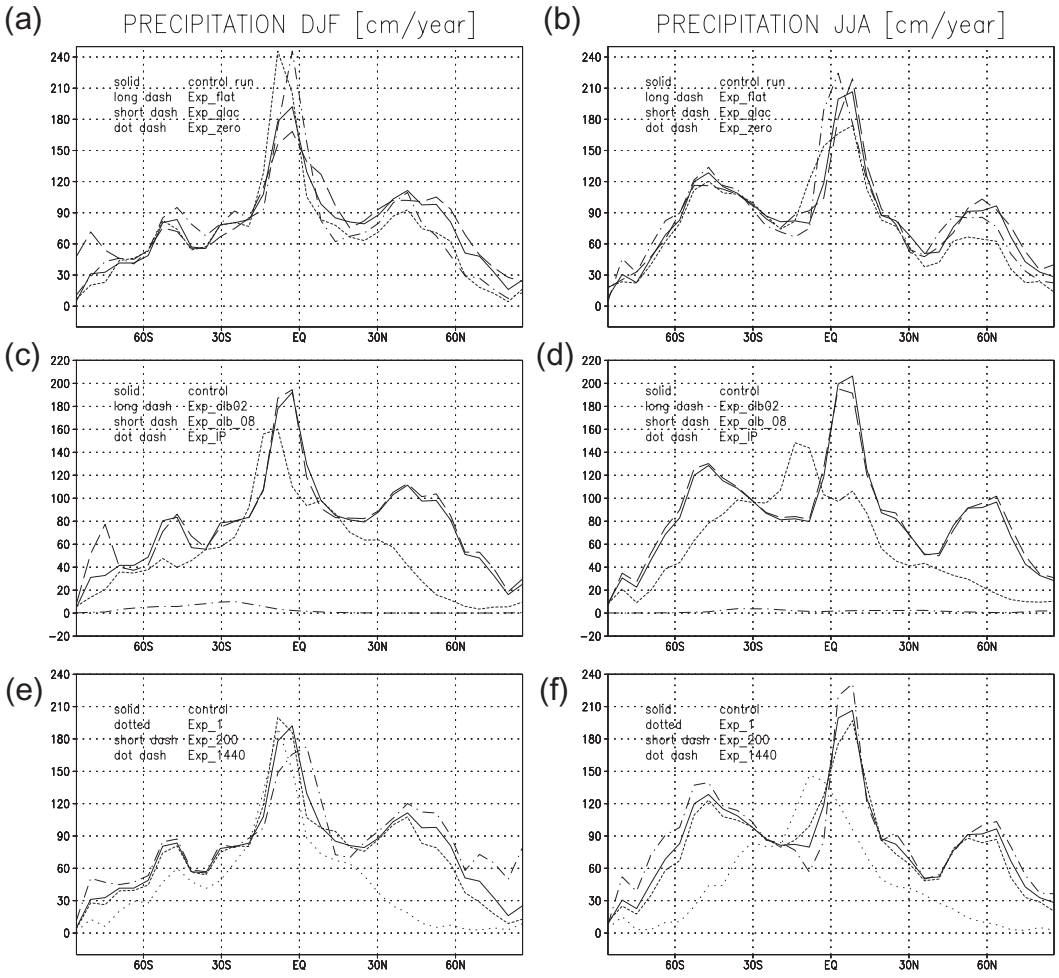

Fig. 9. The DJF and JJA zonal mean precipitation for control run (solid line) and **(a, b)** the experiments investigating the effect of orography and oceanic heat transport; **(c, d)** experiments with changed land albedo and Ice Planet simulation; and **(e, f)** experiments with different CO_2 concentrations.

occurs in the midlatitudes of the NH and SH due to the extensive ice-coverage and negative surface temperatures. The ice-covered planet in EXP_IP prohibits precipitation the whole year round.

The experiment with a fourfold present-day CO_2 concentration shows a decrease in the precipitation during boreal winter and an increase during boreal summer (Fig. 9ef). The tendency is the same as in EXP_flat (described earlier), whereas the experiment with CO_2 equal to 200 ppm exhibits the tendency of EXP_glac – an increase in the precipitation during boreal winter and decrease during boreal summer. Therefore, glacial orography and the reduction of CO_2 act in the same direction. Both change the ITCZ and Hadley circulation in equatorial and tropical latitudes. In experiment EXP_1 the precipitation is considerably lowered, as its maximum does not experience seasonality and is always located in the SH, tending to the same result as in EXP_alb08.

4 Discussions

We investigate the sensitivity of the climate to some extreme boundary and initial conditions and combinations of extreme parameters under present-day insolation and continental distributions. Examining the influence of each factor, we assess the role of the land albedo, the influence of high and low CO_2 concentration levels, the importance of the orography and of the oceanic heat transport.

The experiments with only one parameter changed, show equilibrium states, in which the equatorial ocean remains ice-free. Using a combination of extreme boundary and initial conditions, like zero oceanic heat transport, high land albedo and the initial temperature uniformly set to a value equal to the freezing point, an ice-covered Earth under present-day orbital parameters and CO_2 concentration can be attained. Further investigation of the experiments with a combination of two of the mentioned extreme boundary conditions, shows that the dominant factor for the decrease of temperature in the

ice planet simulation is the land albedo. If the land albedo is a variable parameter, independently of the zero oceanic heat transport or the low initial temperature field, the temperatures increase and tend to reach the values of the control run. Interestingly, the present-day oceanic heat transport alone is not able to produce ice-free equatorial oceans. A full glaciation is delayed but successfully reaches the ice-planet equilibrium (Fig. 4). Even though the heat transport of the present-day climate seems not to be appropriate with respect to ice-covered oceans (Poulsen et al., 2001; Lewis et al., 2003), its role appears to be negligible compared to continental surface properties. Using a 2,5 dimensional coupled climate model of intermediate complexity, Dounadieu et al. (2004) concluded that the dynamic oceanic process cannot prevent the onset of the ice-albedo instability in a Neoproterozoic simulation. Another factor prohibiting the formation of an ice-covered planet is the high initial temperature field (set to present-day values). Although the global temperature falls approximately 20°C, the sea-ice cover advance is restricted up to 30° N and 60° S. The asymmetrical distribution of the sea-ice margins is more sensitive to the paleogeography differences than to the change of other parameters, e.g., the insolation (Poulsen et al., 2002). Releasing the land albedo after the 20-th year of the ice planet simulation (not shown) does not infer any change in the climate system, due to the very low temperatures, which force the land and ice albedo to attain their maximal values. Thus, the ice planet simulation reaches a stable climate and only an external influence can lead to change of this stable state (e.g., increase of carbon dioxide due to strong volcanic activity and lack of chemical weathering).

Does the orography matter in the initiation of extreme climate? The LGM reconstruction of the orography (Peltier, 1994), including the highly elevated Laurentide Ice Sheet, reduces the global temperature by 3°C. The influence of changed orography predominates in the contribution to the Northern Hemispheric cooling, but it is of no importance to the tropics. Thus the altered orography is more important in regional sense, than in global. Jenkins and Frakes (1998) introduced a 2 km north-south mountain chain on the super continent in their Neoproterozoic model set up, and showed that the orogeny could not be considered as a factor for the global glaciation. But it can redistribute the humidity over sea-ice and thus, change the hydrological cycle (Donnadieu et al., 2003). However, the climate system responses nonlinearly to linear change of the height of the ice-sheet (Romanova et al., 2005), which points to the existence of a threshold, over which a runaway albedo feedback over the American continent could be initiated. Further investigation of the sensitivity of the climate system toward enlargement of the Laurentide Ice Sheet could be of interest when searching for this threshold.

The experiments control run, EXP_alb02, EXP_flat, EXP_1440 showed a planetary albedo larger than the surface albedo (in some cases more than 150%), due to the strong evaporation over the ice-free oceans and cloud formation. In the experiments (EXP_alb08, EXPIP_iniTempPD and EXP_1), in which the absolute global temperature is around 0°C and which are characterised by cold climatic conditions and ice-free equatorial and tropical latitudes, the global surface and planetary albedo tend to be in the same order. However, these cold climates (EXP_alb08 and EXP_1) could exhibit an intense equatorial precipitation maxima and a strong Hadley circulation due to the sharp temperature gradients from the equator to the edge of the sea-ice margin, which works against the positive ice-albedo feedback (Bendtsen, 2002). The hydrological cycle and the ITCZ are rather sensitive to the change of the surface temperature in the tropics and to the strength of the Atlantic overturning (Lohmann and Lorenz, 2000; Lohmann, 2003). Interestingly, in the ice-planet experiments EXP_IP and EXPIP_iniIP, the estimates of the global planetary albedo appear smaller than the global surface albedo. On a completely glaciated Earth, the processes of evaporation, cloud formation and precipitation are strongly suppressed or even do not exist, thus the ratio between the incident and reflected short wave radiation on the surface is higher than the ratio between the incident and reflected/scattered short wave radiation on the top of the atmosphere. The loss of energy in the atmosphere could be due to the process of water vapour absorption, where the water vapour is provided only by the process of sublimation.

5 Concluding remarks

Motivated by the early work with EBMs (Budyko, 1969; Sellers, 1969) and the discussion about an ice covered Earth (e.g., Crowley and Baum, 1993; Jenkins and Frakes, 1998; Hyde et al., 2000; Chandler and Sohl, 2000; Crowley et al., 2001; Poulsen et al., 2001; Donnadieu et al., 2002, 2004; Bendtsen, 2002; Lewis et al., 2003; Stone and Yao, 2004), we investigate the possibility for extreme climates under present configurations (continent distribution and orbital forcing) in a simplified AGCM coupled to a mixed layer-sea ice model (Fraedrich, 1998; Franzke et al., 2000; Grosfeld et al., 2006[1]; Romanova et al., 2005).

Investigating the Neoproterozoic glaciations, many authors search for a CO_2 threshold value. Different simulations show a sensitivity of the minimum CO_2 level to continental configurations (Poulsen et al., 2002; Donnadieu et al., 2004), Earth's rotation rate and obliquity (Jenkins and Smith, 1999; Jenkins, 2000), solar luminosity (Crowley et al., 2001) oceanic heat transport (Poulsen et al., 2001) or an increase of the albedo (Lewis et al., 2003). Our experiments for present day setup suggest that the reduction of atmospheric CO_2 alone is not sufficient to provoke global glaciation under present-day insolation. We find a strong nonlinearity in the NH at a CO_2 concentration of 25 ppm. The temperature anomaly, relative to the present-day simulation, can reach –40°C at 1 ppm. Our simulations show that the ini-

tial condition of the system is important when simulating a snowball Earth. Indeed, a hysteresis of the climate system is found with respect to a change of the infrared forcing (Crowley et al., 2001) and solar constant (Stone and Yao, 2004). We suppose similar climate behaviour to a slow change of the CO_2 concentration and a snow cover and we will address this question in our further research.

In our sensitivity experiments we evaluated extreme effects of land albedo and CO_2 on climate in a similar way as Fraedrich et al. (1999) for vegetation extremes on the atmosphere. In our approach, we calculated the sea surface temperature interactively by assuming different ocean heat transports. We have neglected several climatic links between the components, including e.g., the hydrological cycle/temperature, vegetation, weathering rates, carbon cycle, and deep ocean circulation. As a logical next step, more interactive climate components will be included in order to estimate the most extreme climate states under present and past climate configurations. The combined effects yield different regimes which are relevant to understand past climate evolutions as recorded, e.g., in cabonate deposites.

Acknowledgements. We gratefully acknowledge the suggestions and recommendations of F. Lunkeit and thank K. Fraedrich for providing us with the model code. We thank also M. Dima and K. Vosbeck for the improvement of the manuscript. This work has been funded by the German Ministry for Education and Research (BMBF) within DEKLIM project "Climate Transitions" and MARCOPOLI.

Edited by: V. Masson-Delmotte

References

Bendtsen, J.: Climate sensitivity to changes in solar insolation in a simple coupled model, Clim. Dyn., 18, 595–609, 2002.

Berger, A. L.: Long term variations of daily insolation and quaternary climatic changes, J. Atmos. Sci., 35(12), 2362–2367, 1978.

Budyko, M. I.: The effect of solar radiation variations on the climate of the Earth, Tellus, 21, 611–619, 1969.

Budyko, M. I.: The Earth's climate: past and future, Academic Press, New York, p. 307, 1982.

Butzin, M., Prange, M., and Lohmann, G.: Studien zur 14C-Verteilung im glazialen Ozean mit einem globalen Ozeanzirkulationsmodell, Terra Nostra, 6, 86–88, 2003.

Butzin, M., Prange, M., and Lohmann G.: Radiocarbon simulations for the glacial ocean: the effects of wind stress, Southern Ocean sea ice and Heinrich events, Earth Planet. Sci. Lett., 235, 45–61, doi:10.1016/j.epsl.2005.03.003, 2005.

Caldeira, K. and Kasting, J. F.: The life span of the biosphere revisited, Nature, 360, 721–723, 1992.

Chandler, M. A. and Sohl, L. E.: Climate forcings and the initiation of low-latitude ice sheets during Neoproterozoic Varanger glacial interval, J. Geophys. Res., 105, 20 737–20 756, 2000.

Claussen, M., Mysak, L. A., Weaver, A. J., Crucifix, M., Fichefet, T., Loutre, M. F., Weber, S. L., Alcamo, J., Alexeev, V. A., Berger, A., Calov, R., Ganopolski, A., Goosse, H., Lohmann, G., Lunkeit, F., Mokhov, I. I., Petoukhov, V., Stone, P., and Wang, Z.: Earth system models of intermediate complexity: Closing the gap in the spectrum of climate system models, Clim. Dyn., 18, 579–586, 2002.

CLIMAP Project Members: Seasonal reconstructions of the earth's surface at the Last Glacial Maximum, Geological Society of America, Map and Chart Series, MC-36, 18, 18 maps, 1981.

Crowley, T. J. and Baum, S. K.: Effects of decreased solar luminosity on Late Precambrian ice extent, J. Geophys. Res., 98, 16 723–16 732, 1993.

Crowley, T. J., Hyde, W. T., and Peltier, W. R.: CO_2 levels required for deglaciation of a 'Near Snowball' Earth, Geophys. Res. Lett., 28, 283–286, 2001.

Donnadieu, Y., Ramstein, G., Fluteau, F., Besse, J., and Meert, J.: Is high obliquity a plausible cause for Neproterozoic glaciations?, Geophys. Res. Lett., 29, doi:10.1029/2002GL015902, 2002.

Donnadieu, Y., Fluteau, F., Ramstein, G., Ritz, C., and Besse, J.: Is there a conflict between the Neoproterozoic glacial deposits and snowball Earth interpretation: an improved understanding with numerical modeling, Earth Plan. Sci. Lett., 208, 101–112, 2003.

Donnadieu, Y., Ramstein, G., Fluteau, F., Roche, D., and Ganopolski, A.: The impact of atmospheric and oceanic heat transports on the sea-ice-albedo instability during the Neoproterozoic, Clim. Dyn., 22, 293–306, 2004.

Eliasen, E., Machenhauer, B., and Rasmussen, E.: On a numerical method for integration of the hydrodynamical equations with a spectral representation of the horizontal fields, Report No. 2, Institute for Theoretical Meteorology, University of Copenhagen, 37 pp., 1970.

Evans, D. A. D., Li, Z. X., Kirschvink, J. L., and Wingate, M. T. D.: A high-quality mid-Neoproterozoic paleomagnetic pole from South China, with implications for ice ages and the breakup configuration of Rodinia, Precambrian Res., 100(1–3), 313–334, 2000.

Fraedrich, K., Kirk, E., and Lunkeit, F.: Portable University Model of the Atmosphere, Deutsches Klimarechenzentrum, Tech. Rep., 16, 377 pp., 1998.

Fraedrich, K., Kleidon, A., and Lunkeit, F.: A green planet versus a desert world: Estimating the effect of vegetation extremes on the atmosphere, J. Climate, 12, 3156–3163, 1999.

Franzke, C., Fraedrich, K., and Lunkeit, F.: Low frequency variability in a simplified atmospheric global circulation model: Storm track induced 'spatial resonance', Quat. J. Roy. Met. Soc., 126, 2691–2708, 2000.

Frisius, T., Lunkeit, F., Fraedrich, K., and James, I. N.: Storm-track organization and variability in a simplified atmospheric global circulation model (SGCM), Quat. J. Roy. Met. Soc., 124, 1019–1043, 1998.

Hoffman, P. F. and Schrag, D. P.: The snowball Earth hypothesis: testing the limits of global change, Terra Nova, 14, 129–155, 2002.

Hoffman, P. F., Kaufman, A. J., Halverson, G. P., and Scharg, D. P.: A Neoproterozoic snowball earth, Science, 281, 1342–1346, 1998.

Hyde, W. T., Crowley, T. J., Baum, S. K., and Peltier, W. R.: Neoproterozoic "snowball Earth" simulations with a coupled climate/ice-sheet model, Nature, 405, 425–429, 2000.

Jenkins, G. S.: Global climate model high-obliquity solutions to the ancient climate puzzles of the Faint Young Sun Paradox and

low altitude Proterozoic Glaciation, J. Geophys. Res., 105, 7357–7370, 2000.

Jenkins, G. S. and Frakes, L. A.: GCM sensitivity test using increased rotation rate, reduced solar forcing and orography to examine low latitude glaciation in the Neoproterozoic, Geophys. Res. Lett., 25, 3525–3528, 1998.

Jenkins, G. S. and Smith, S. R.: GCM simulation of Snowball Earth conditions during the late Proterozoic, Geophys. Res. Lett., 26, 2263–2266, 1999.

Kirschvink, J. L.: Late proterozoic low-lattitude global glaciation: the Snowball Earth, in: The Proterozoic biosphere, edited by: Schopf, J. W. and Klein, C., Cambridge UK, pp 51–52, 1992.

Kirschvink, J. L., Gaidos, E. J., Bertani, E., Beukes, N. J., Gutzmer, J., Maepa, L. N., and Steinberger, R. E.: Paleoproterozoic snowball Earth: Extreme climatic and geochemical global change and its biological consequences, PNAS 97, 1400-14005, 2000.

Kleidon, A., Fraedrich, K., and Heimann, M.: A green planet versus a desert world: Estimating the maximum effect of vegetation on the surface energy balance, Climatic Change, 44, 471–493, 2000.

Kubatzki, C. and Claussen, M.: Simulation of the global biogeophysical interactions during the Last Glacial Maximum, Climate Dynamics, 14, 461–471, 1998.

Langen, P. L. and Alexeev, V. A.: Multiple equilibria and asymmetric climates in the CCM3 coupled to an oceanic mixed layer with thermodynamic sea ice, Geophys. Res. Lett., L04201, 2004.

Lewis, J. P., Weaver, A. J., Johnston, S. T., and Eby, M.: Neoproterozoic "snowball Earth": Dynamic sea ice over a quiescent ocean, Paleoceanography, 18, doi:10.1029/2003PA000926, 2003.

Lohmann, G.: Atmospheric and oceanic freshwater transport during weak Atlantic overturning circulation, Tellus, 55 A, 438–449, 2003.

Lohmann, G. and Lorenz, S.: On the hydrological cycle under paleoclimatic conditions as derived from AGCM simulations, J. Geophys. Res., 105, 417–436, 2000.

Lorenz, S., Grieger, B., Helbig, Ph., and Herterich, K.: Investigating the sensitivity of the atmospheric general circulation model ECHAM 3 to paleoclimatic boundary conditions, Geol. Rundsch., 85, 513–524, 1996.

Lunkeit, F., Bauer, S. E., and Fraedrich, K.: Storm tracks in a warmer climate: Sensitivity studies with a simplified global circulation model, Clim. Dyn., 14, 813–826, 1998.

Macdonald, A. M. and Wunsch, C.: An estimate of global ocean circulation and heat fluxes, Nature, 382, 436–439, 1996.

Manabe, S. and Bryan, K.: CO_2-induced change in a coupled ocean-atmosphere model and its paleo-climatic implications, J. Geophys. Res., 90, 11 689–11 707, 1985.

Oglesby, R. and Saltzman, B.: Sensitivity of the equilibrium surface temperature of a GCM to systematic changes in atmospheric carbon dioxide, Geophys. Res. Lett., 17, 1089–1092, 1990.

Orszag, S. A.: Transform method for calculation of vector-coupled sums: Application to the spectral form of the vorticity equation, J. Atmos. Sci., 27, 890–895, 1970.

Peltier, W. R.: Ice age paleotopography, Science, 265, 195–201, 1994.

Pflaumann, U., Sarnthein, M., Chapman, M., d'Abreu, L., Funnell, B., Huels, M., Kiefer, T., Maslin, M., Schulz, H., Swallow, J., van Kreveld, S., Vautravers, M., Vogelsang, E., Weinelt, M.: Glacial North Atlantic: Sea-surface conditions reconstructed by GLAMAP 2000, Paleoceanography, 18(3), 1065, doi:10.1029/2002PA000774, 2003.

Phillips, T. J., Anderson, R., and Brösius, M.: Hypertext summary documentation of the AMIP models, UCRL-MI-116384, Lawrence Livermore National Laboratory, Livermore, CA, 1995.

Poulsen, C. J., Pirrehumbert, R. T., and Jacob, R. L.: Impact of ocean dynamics on the simulation of the Neoproterozoic "snowball Earth", Geophys. Res. Lett., 28, 1575–1578, 2001.

Poulsen, C. J., Jacob, R. L., Pierrehumbert, R. T., and Huynh, T. T.: Testing paleogeographic controls on a Neoproterozoic snowball Earth, Geophys. Res. Lett., 29, doi:10.1029/2001GL014352, 2002.

Poulsen, C. J.: Absence of runaway ice-albedo feedback in the Neoproterozoic, Geology, 31, 473–476, 2003.

Roeckner, E., Arpe, K., Bengtsson, L., Brinkop, S., Dümenil, L., Esch, M., Kirk, E., Lunkeit, F., Ponater, M., Rockel, B., Sausen, R., Schlese, U., Schubert, S., and Windelband, M.: Simulation of present-day climate with the ECHAM model: Impact of model physics and resolution. MPI Report No. 93, ISSN 0937-1060, Max-Planck-Institut für Meteorologie, Hamburg, Germany, 171 pp., 1992.

Romanova, V., Lohmann, G., Grosfeld, K., and Butzin, M.: The relative role of oceanic heat transport and orography on glacial climate, Quat. Sci. Rev., doi:10.1016/j.quascirev.2005.07.007, 2005.

Schmidt, P. W. and Williams, G. E.: The Neoproterozoic climatic paradox; equatorial palaeolatitude for Marinoan Glaciation near sea level in South Australia, Earth Planet. Sci. Lett., 134(1–2), 107–124, 1995.

Sellers, W. D.: A global climatic model based on the energy balance of the earth atmosphere system, J. Appl. Meteorol., 8, 392–400, 1969.

Sohl, L. E., Christie-Blick, N., and Kent, D. V.: Paleomagnetic polarity reversals in Marinoan (ca. 600 Ma) glacial deposits of Australia: implications for the duration of low-latitude glaciation in Neoproterozoic time, Geol. Soc. Am. Bull., 111(8), 1120–1139, 1999.

Stone, P. H. and Yao, M. S.: The ice-covered Earth instability in a model of intermediate complexity, Clim. Dyn., 22, 815–822, doi:10.1007/s00382-004-0408-y, 2004.

Wyputta, U. and McAvaney, B. J.: Influence of vegetation changes during the Last Glacial Maximum using the BMRC atmospheric general circulation model, Clim. Dyn., 17, 923–932, 2001.